

Homogeneous Catalysis

Kinetic Studies on the Palladium(II)-Catalyzed Oxidative Cross-Coupling of Thiophenes with Arylboron Compounds and Their Mechanistic Implications

Ingo Schnapperelle, Stefan Breitenlechner,* and Thorsten Bach*[a]

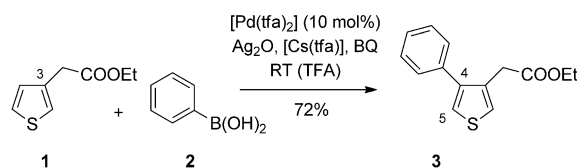
Abstract: Reaction orders for the key components in the palladium(II)-catalyzed oxidative cross-coupling between phenylboronic acid and ethyl thiophen-3-yl acetate were obtained by the method of initial rates. It turned out that the reaction rate not only depended on the concentration of palladium trifluoroacetate (reaction order: 0.97) and phenylboronic acid (reaction order: 1.26), but also on the concentration of the thiophene (reaction order: 0.55) and silver oxide (reaction order: -1.27). NMR spectroscopy titration studies established the existence of 1:1 complexes between the silver salt and both phenylboronic acid and ethyl thiophen-3-yl acetate. A low inverse kinetic isotope effect (k_H/k_D

$k_D = 0.93$) was determined upon employing the 4-deuterated isotopomer of ethyl thiophen-3-yl acetate and monitoring its reaction to the 4-phenyl-substituted product. A Hammett analysis performed with *para*-substituted 2-phenylthiophenes gave a negative ρ value for oxidative cross-coupling with phenylboronic acid. Based on the kinetic data and additional evidence, a mechanism is suggested that invokes transfer of the phenyl group from phenylboronic acid to a 1:1 complex of palladium trifluoroacetate and thiophene as the rate-determining step. Proposals for the structure of relevant intermediates are made and discussed.

Introduction

Palladium-catalyzed C–H activation reactions at arenes have attracted enormous attention in recent years because they allow for regio- and chemoselective substitution reactions, which are otherwise difficult to achieve.^[1] Arylation reactions at arenes can be performed upon palladium catalysis by either employing aryl halides^[2] or aryl metal compounds, for example, arylboronic acids (oxidative cross-coupling).^[3] In the latter case, a stoichiometric oxidant is normally required to regenerate Pd^{II} from Pd⁰, which is produced in the C–C bond-formation process by reductive elimination. Although extensive experimental data have been accumulated in the field of oxidative cross-coupling reactions, detailed kinetic experiments have rarely been conducted nor have these data been extensively employed to support mechanistic proposals.^[4] In general, the composition of the reaction mixture, which often consists—apart from substrate—of three or more ingredients, hampers the generation and interpretation of kinetic data. In 2011, we began investigating the oxidative arylation of thiophenes with arylboronic acids^[5] and were particularly intrigued by the high regioselectivity of these reactions.^[6] Typical reaction conditions for this transformation included the use of palladium trifluor-

oacetate (Pd(tfa)₂) as the catalyst (10 mol%) and silver oxide (Ag₂O) as the oxidant (2.0 equiv). Trifluoroacetic acid (TFA) served as the solvent. 1,4-Benzoquinone (BQ; 0.5 equiv) and cesium trifluoroacetate (Cs(tfa)) (1.0 equiv) were used as additives ($c = 0.2$ M). A prototypical example for this reaction is the conversion of ethyl thiophen-3-yl acetate (**1**) into product **3** by employing phenylboronic acid (**2**) as the arylating reagent (2.0 equiv) at ambient temperature (Scheme 1). The depicted



Scheme 1. Regioselective Pd^{II}-catalyzed oxidative cross-coupling of **2** with **1**.

4-substituted thiophene was formed as essentially a single regioisomer (regioisomeric ratio (r.r.) = 97:3). In further experiments, the same regioselectivity preference was found also for other 2-substituted thiophenes, for 3- and 2,3-disubstituted thiophenes, as well as for benzothiophene.^[7] In addition, it was found that the choice of the acidic solvent needed to be adjusted to the reactivity of the thiophene, with more electron-rich thiophenes requiring mixtures of HOAc/TFA as a solvent instead of neat TFA.

Apart from synthetic applications of this method to the synthesis of new materials,^[8] we have also investigated the mech-

[a] Dr. I. Schnapperelle, Dr. S. Breitenlechner, Prof. Dr. T. Bach
Department Chemie and Catalysis Research Center (CRC)
Technische Universität München, Lichtenbergstraße 4
85747 Garching (Germany)
E-mail: thorsten.bach@ch.tum.de

Supporting information for this article is available on the WWW under
<http://dx.doi.org/10.1002/chem.201503067>.

anistic course of the reactions. Preliminary results had indicated that an electrophilic palladium species could be the reactive intermediate, which attacked position C5 prior to C–C bond formation at C4.^[5] In related work, starting with seminal contributions by the groups of Studer and Itami,^[3c] similar regioselectivities have been observed for oxidative cross-coupling reactions at thiophenes.^[3] Transmetalation from the arylating agent to palladium has been postulated to precede an attack at the thiophene ring.^[9] Calculations on a cationic $[\text{Pd}(\text{bipy})\text{Ph}]^+$ complex (bipy = 2,2'-bipyridine) have suggested that C–C bond formation occurs by a carbopalladation pathway, in the course of which the aryl–thiophene bond is formed at position C4(C3) and palladium is linked to carbon atom C5(C2).^[10] In the same study, it was hypothesized that the subsequent deprotonation of the intermediate was rate limiting, whereas carbopalladation was said to be reversible. Subsequent publications on the topic reiterated this mechanistic proposal.^[3d,e]

We have now performed extensive kinetic studies on the reaction $1 \rightarrow 3$, which are presented herein. Additional mechanistic information was obtained from the determination of kinetic isotope effects (KIEs), from equilibrium studies and from a Hammett analysis.

Results

Initial work was directed towards a kinetic analysis of the reaction under reproducible homogenous conditions. Homogeneity was secured by pretreating the reaction mixture with ultrasound prior to addition of **2**. The reaction order of each component was determined by using the method of initial rates^[11] (see the Supporting Information for further details).

Kinetic studies

The reactions were performed under standard conditions, that is, at a substrate concentration of $c = 0.2 \text{ M}$ in TFA (2.5 mL). All other reagents were used in the equivalents mentioned above (unless their respective concentration was varied; see below).

Upon variation of the $\text{Pd}(\text{tfa})_2$ concentration (2.0 to 10.0 mol%), a linear rate dependence was observed (Figure 1a). The reaction order was 0.97, as determined from the fitting procedure by the method of least squares. The reaction order for the concentration of

1 (Figure 1b) was also positive, but there was no linear relationship. An unbiased analysis generated a calculated reaction order of 0.55, although one could potentially also identify two different linear regimes (0.0–0.2 and 0.2–0.5 M). Due to solubility issues, the concentration of **2** could only be varied in the range of 0.2 to 0.6 M. In this concentration range, the reaction rate seems to depend linearly on the **2** concentration (Figure 1c). However, the calculated reaction order is 1.26 once the origin of the coordinate system is considered. The reaction order shows clearly a negative relationship to the concentration of Ag_2O (Figure 1d) and was determined to be -1.27 . It should be noted that the presence of Ag_2O is mandatory to ensure the desired chemo- and regioselectivity of arylation. If performed in the absence of a silver source, the oxidative cross-coupling reaction proceeded sluggishly in heterogeneous solution and resulted in a mixture of regioisomers.^[5] It can be assumed that, upon dissolution, Ag_2O reacts with TFA to form the respective trifluoroacetate salt $[\text{Ag}(\text{tfa})]$. The simultaneously formed water has no influence on the reaction rate, as shown in separate experiments, in which water was systematically added to the reaction mixture. The influence of the concentration of BQ on the rate was marginal. There was a slightly negative reaction order, which indicated possible complexation of BQ to the catalytically active Pd complex (see below). However, if BQ was completely omitted, the reaction stopped at low

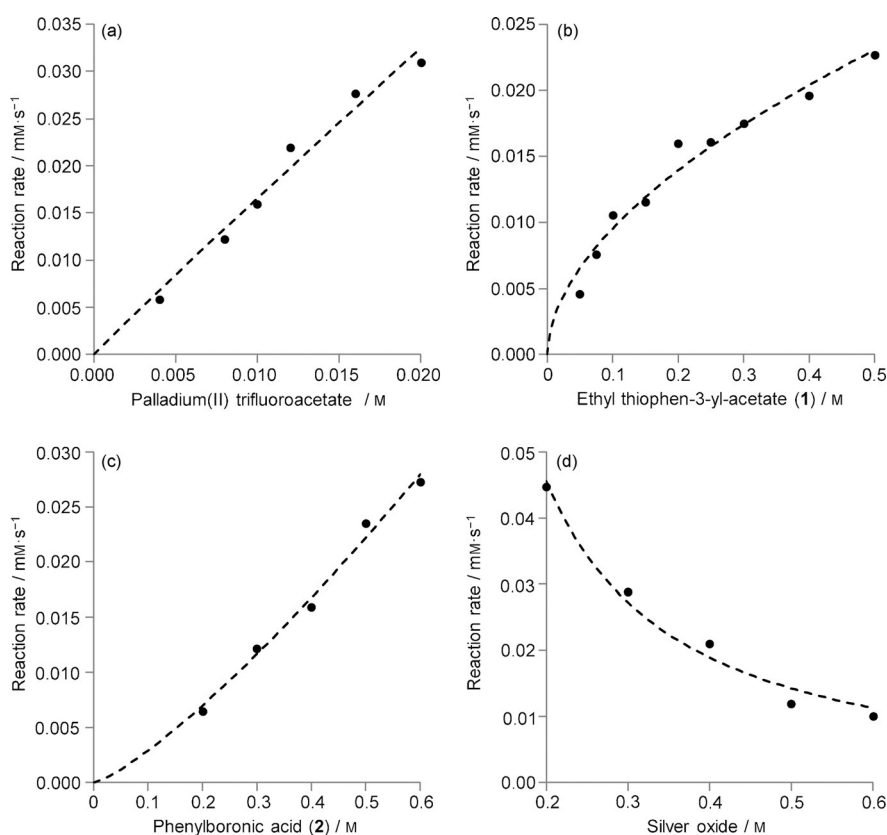


Figure 1. Experimental data (●) and best fit curves (---) calculated from the empirical rate law for the reaction rates with varying concentrations of different components: a) $\text{Pd}(\text{tfa})_2$, b) **1**, c) **2**, d) Ag_2O . For further details, see the text and Supporting Information.

conversion. The experimentally determined reaction rate for the formation of **3** can be empirically summarized by Equation (1). The curves shown in Figure 1 are mathematically derived from the respective exponential rate equation, $f([\text{reagent}]) = k[\text{reagent}]^x$, for the respective reagents $\text{Pd}(\text{tfa})_2$, **1**, **2**, and Ag_2O .

$$\frac{d[\mathbf{3}]}{dt} = k[\text{Pd}(\text{tfa})_2]^{0.97}[\mathbf{1}]^{0.55}[\mathbf{2}]^{1.26}[\text{Ag}_2\text{O}]^{-1.27}[\text{BQ}]^{-0.13} \quad (1)$$

Equilibrium studies

The negative reaction order for Ag_2O raised the question of whether silver ions would form complexes with the substrate and reagents of oxidative cross-coupling. The formation of a complex of **2** with Ag_2O was indicated by the fact that the presence of the latter improved the solubility of the former. If the Ag_2O concentration was decreased below 0.2 M, a precipitate of **2** was observed. ^1H NMR spectroscopy titration experiments were initially attempted with $\text{Ag}(\text{tfa})$ and **2** in TFA. However, the limited solubility of **2** precluded the observation of the complex at low $\text{Ag}(\text{tfa})$ concentrations. The titration data were therefore recorded in a mixture of TFA/ H_2O (10:1 v/v) with $[\text{D}_6]$ DMSO as an external standard. A Job plot analysis^[12] (Figure 2a) revealed a 1:1 stoichiometry for the putative complex **2**/ $\text{Ag}(\text{tfa})$. The association constant was determined to be 30 M^{-1} (Figure 2b).

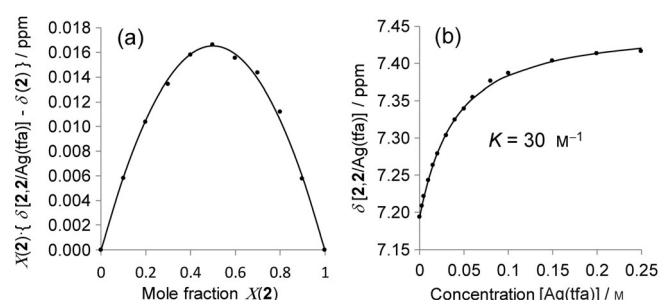


Figure 2. a) Job plot for the complex of **2** and silver trifluoroacetate. b) Determination of the equilibrium constant, K , from the reaction of **2** with silver trifluoroacetate.

Under the same conditions, a ^1H NMR spectroscopy titration was performed with **1** and $\text{Ag}(\text{tfa})$. Remarkably, not only was the existence of a 1:1 complex of **1**/ $\text{Ag}(\text{tfa})$ corroborated by Job plot analysis (Figure 3a), it was also found that the association of the silver ion to the thiophene was relatively strong. The association constant was higher than the association constant of **2**/ $\text{Ag}(\text{tfa})$ and was determined to be 76 M^{-1} . The most significant ^1H NMR shift differences were observed for hydrogen atoms attached to C5 ($\Delta\delta = 0.16 \text{ ppm}$), C4 ($\Delta\delta = 0.12 \text{ ppm}$), and C2 ($\Delta\delta = 0.12 \text{ ppm}$) of the thiophene. Values in brackets correspond to $\Delta\delta$, which was consistently observed at a lower field, at an equimolar concentration of $\text{Ag}(\text{tfa})$. The chemical shifts of the other protons of the side chain were only minimally affected by the addition of $\text{Ag}(\text{tfa})$.

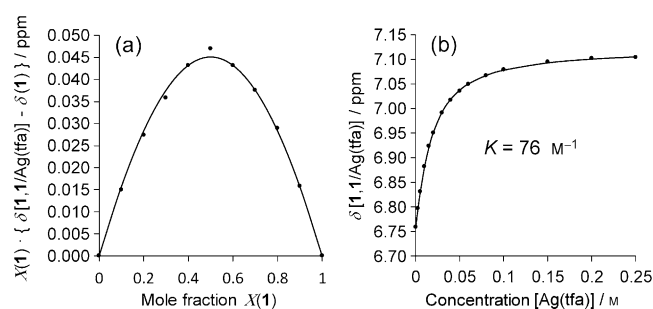
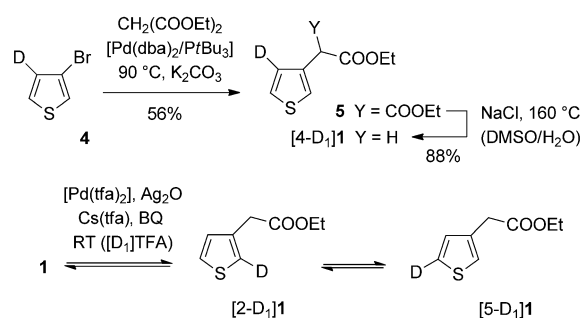


Figure 3. a) Job plot of **1** and silver trifluoroacetate. b) Determination of the equilibrium constant, K , from the reaction of **1** with silver trifluoroacetate.

Kinetic isotope effect (KIE)

Deuterated 3-bromothiophene (**4**) was accessible from 3,4-dibromothiophene by magnesium–bromine exchange and subsequent hydrolysis in $\text{D}_2\text{O}/\text{D}_2\text{SO}_4$ (Scheme 2). Ensuing substitution of bromide was performed with diethyl malonate under palladium(0) catalysis. The resulting diester **5** was selectively decarboxylated under Krapcho conditions^[13] to give the 4-deuterated product $[4\text{-D}_1]\mathbf{1}$. The deuterium content was deter-



Scheme 2. Preparation of monodeuterated ethyl thiophen-3-yl acetate $[4\text{-D}_1]\mathbf{1}$ (top); dba = dibenzylideneacetone. The isomers $[2\text{-D}_1]\mathbf{1}$ and $[5\text{-D}_1]\mathbf{1}$ show a fast H/D exchange under the oxidative cross-coupling conditions (bottom).

mined to be $>99\%$ by ^1H NMR spectroscopy and gas liquid chromatography mass spectrometry (GLC-MS) analysis. The monodeuterated thiophenes $[2\text{-D}_1]\mathbf{1}$ and $[5\text{-D}_1]\mathbf{1}$ were not suitable for KIE studies. It was shown that H/D exchange at positions C2 and C5 of thiophene **1** was rapid under the reaction conditions. Treatment of **1** with $[\text{D}_1]\text{TFA}$ in the absence of **2** led, after 3 h, to deuterium incorporation of 21% at the 2-position and 73% at the 5-position (Scheme 2).

The most accurate value for the KIE was obtained by performing an intermolecular competition experiment.^[14] To this end, equimolar amounts of **1** and $[4\text{-D}_1]\mathbf{1}$ were subjected to the reaction conditions of the oxidative cross-coupling with **2** (see Scheme 1). The isotopomer ratio of the product was determined by GLC-MS analysis (selected ion monitoring mode). Figure 4 shows the double logarithmic plot for the determination of $k_{\text{H}}/k_{\text{D}}$ and the conversion profile for this reaction. The KIE was determined as 0.93. The order of magnitude of this

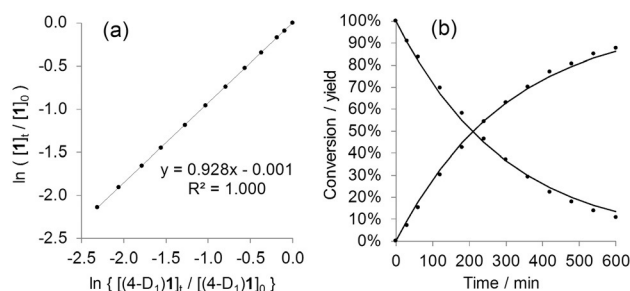
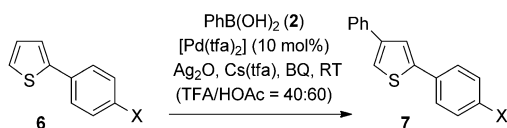


Figure 4. a) Double logarithmic plot for the determination of the KIE. b) Conversion of **1** and formation of product **3**.

value (± 0.10) was confirmed by separate measurements of the absolute rate constants.

Hammett plot

As previously pointed out, the oxidative cross-coupling protocol is applicable to 2- and 3-substituted thiophenes. The 2-phenylthiophenes **6** seemed suited to study the relative rate constants of the reactions, depending on the respective *para*-substituent X. The reaction of the parent compound **6a** (X=H) proceeds regioselectively (Scheme 3) and delivers the respective substitution product **7a** in a yield of 86%.^[7] The preferred solvent mixture for this transformation was TFA in HOAc (40:60 v/v).



Scheme 3. Reaction of various *para*-substituted 2-phenylthiophenes **6** with **2** under standard conditions. For the influence of the *para*-substituent X on the relative rate constants, see Figure 5.

Because the reaction occurs at position C4, steric effects were assumed to be negligible and the electronic influence of X was assessed by Hammett analysis. Intermolecular competition experiments were performed in TFA/HOAc (40:60 v/v) and the relative rate constants were determined by GLC analysis. The best linear fit was obtained when the relative rate was plotted against $\sigma_p + r(\sigma^+ - \sigma_p)$.^[15] The ρ value obtained from this plot was negative (-1.19) with $r=0.18$ (Figure 5). If the relative rates were plotted against σ_p , the ρ value was slightly more negative ($\rho = -1.29$).

Additional mechanistic experiments

¹H NMR spectroscopy experiments were performed with Pd(tfa)₂ and the individual reaction components **1** and **2**. When treating thiophene **1** ($c=0.2$ M) with an equimolar amount of Pd(tfa)₂ in TFA/H₂O (10:1 v/v), a precipitate remained, which seemed to further dissolve after an extended

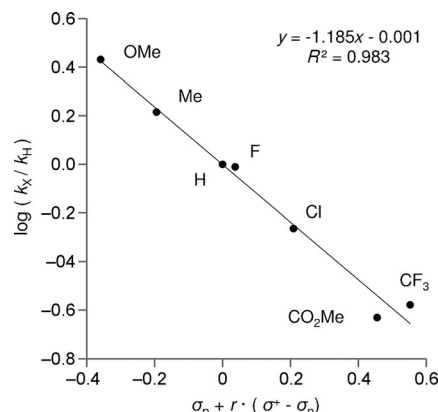
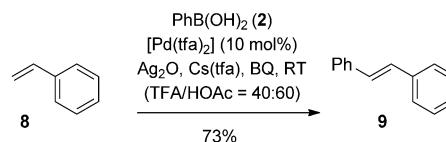


Figure 5. Hammett plot used to calculate the reaction constant ρ from the slope of the line of best fit.

period of time. An upfield shift of all thiophene protons ($\Delta\delta \approx 0.1$ ppm after 9 h) was observed in the ¹H NMR spectrum. In addition, a new species was detected, which showed only two doublets ($J(\text{H,H})=5.3$ Hz) for the thiophene protons. The spectrum remained essentially unchanged after an additional 18 h. Due to the insolubility of Pd(tfa)₂ at higher concentrations, an association constant could not be determined. Upon exposure of **1** to equimolar Pd(tfa)₂ at lower concentration ($c=0.01$ M), a similar set of new signals (two doublets) was observed, but no chemical shift change was detected for the thiophene protons. Moreover, the thiophene started to degrade rapidly to a mixture of unidentifiable products.

Upon adding stoichiometric amounts of Pd(tfa)₂ to a homogeneous solution of **2** ($c=0.01$ M) in TFA/H₂O (10:1 v/v), compound **2** was shown to undergo, according to a zero-order rate law, a conversion to biphenyl, benzene, and traces of phenol. No further species could be identified by ¹H NMR spectroscopy. These results seemed to indicate that transmetalation of **2** to Pd(tfa)₂ was a viable pathway under the reaction conditions of oxidative cross-coupling. The formation of biphenyl and benzene was ascribed to a rapid consecutive reaction of an intermediate phenyl palladium species. To confirm that this species was a competent intermediate for a subsequent carbometalation reaction, an oxidative Heck-type reaction^[16] was performed. When styrene (**8**) was treated with **2** under typical conditions previously employed for the oxidative cross-coupling reaction, (*E*)-stilbene (**9**) was isolated in 73% yield (Scheme 4).



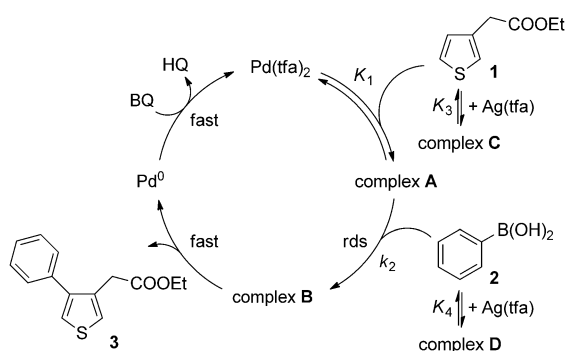
Scheme 4. Heck-type reaction of **8** with **2** under the reaction conditions of oxidative cross-coupling. The only isolable product was **9**.

Discussion

There is no simple mechanistic scheme that immediately follows from the determined reaction orders. The first-order rate law observed for $\text{Pd}(\text{tfa})_2$ can be expected based on its pivotal role as a homogeneous catalyst of cross-coupling. The rate diagram for **1** resembles the rate diagram of reactions that occur in a catalyst saturation regime (Michaelis–Menten kinetics). Indeed, an association of $\text{Pd}(\text{tfa})_2$ to thiophene **1** can be deduced from NMR spectroscopy experiments performed in the concentration range of the catalytic reaction ($c=0.2\text{ M}$). Contrary to typical reactions following Michaelis–Menten kinetics,^[17] the reaction cannot be productive without a third component—apart from catalyst and substrate. Boronic acid **2** is required to deliver the phenyl group, which will eventually be bound to the thiophene. If the attack of **2** was rate determining, the reaction order relative to **2** would be unity. Inspection of the rate diagram of **2** (Figure 1c) reveals that the graph is indeed linear, but does not intersect the origin of the coordinate system. A possible reason for this discrepancy could be argued to be the association of **2** to $\text{Ag}(\text{tfa})$, as unequivocally established by NMR spectroscopy titration experiments (Figure 2). On the other hand, the coordination of $\text{Ag}(\text{tfa})$ to both **2** and thiophene **1** accounts for the negative reaction order of Ag_2O (Figure 1d). Based on the rate data and equilibrium studies, the situation can be summarized as depicted in Scheme 5. Association of $\text{Ag}(\text{tfa})$ to the reaction components leads to equilibria that limit the availability of these species for the catalytic cycle. An equilibrium between $\text{Pd}(\text{tfa})_2$ and thiophene **1** to complex **A** predates the rate-determining step (rds), that is, the attack of **2** at complex **A**. Formation of complex **B** is followed by further rapid reactions, which lead to product development and catalyst regeneration.

If we take the picture depicted in Scheme 5 as a starting point for the interpretation, we arrive at a rate law [Eq. (2)] in which the equilibrium concentrations, $[\mathbf{1}]_{\text{eq}}$ and $[\mathbf{2}]_{\text{eq}}$, need to be calculated from the respective equilibria to complexes **C** and **D** (see the Supporting Information for further details).

$$\frac{d[\mathbf{3}]}{dt} = \frac{k_2[\text{Pd}(\text{tfa})_2][\mathbf{1}]_{\text{eq}}[\mathbf{2}]_{\text{eq}}}{K_1^{-1} + [\mathbf{1}]_{\text{eq}}} \quad (2)$$



Scheme 5. Mechanistic proposal to explain the unusual reaction orders for **2** and Ag_2O (HQ = 1,4-hydroquinone).

Based on the method of least squares as a regression analysis tool, we achieved a global fit of the experimental data to the calculated reaction rates, from which values for K_1 , k_2 , K_3 , and K_4 were obtained mathematically. With these values, the calculated best fit curves were superimposed on the data points that were experimentally obtained (Figure 6). Within the concentration range of our measurements, the curves coincide with the experimental values.

The global fit analysis delivered an equilibrium constant of $K_1=15\text{ M}^{-1}$ for the complexation of thiophene **1** to $\text{Pd}(\text{tfa})_2$. From Equation (2), it is evident that, in a situation in which $K_1^{-1} > [\mathbf{1}]_{\text{eq}}$, the reaction order for thiophene **1** becomes unity, as observed in the low concentration range (0.0–0.2 M). If $[\mathbf{1}]_{\text{eq}}$ becomes large, that is, at high concentration (0.2–0.5 M), the reaction order for thiophene **1** approaches zero (Figure 6b). For **2**, the previous assumption that coordination to $\text{Ag}(\text{tfa})$ leads to a significant deviation of $[\mathbf{2}]_{\text{eq}}$ from $[\mathbf{2}]$ at low concentration rate was corroborated by the regression analysis (Figure 6c). The concentration of $\text{Ag}(\text{tfa})$ or Ag_2O , respectively, does not directly appear in Equation (2), but is implicitly included in the values of $[\mathbf{1}]_{\text{eq}}$ and $[\mathbf{2}]_{\text{eq}}$. Solutions to the cubic equation, with which $[\text{Ag}(\text{tfa})]_{\text{eq}}$ can be calculated, were found algebraically. The curve form $f(x)=x^{-n}$ for the rate diagram of Ag_2O (Figure 6d) can be explained by appropriate approximation.

From the KIE experiments, it is evident that the C–H bond at position C4 of the thiophene is not broken in the rds. In other words, the C4–H bond is fully intact in complexes **A** and **B**. The inverse KIE could be tentatively interpreted as a hybridization change at position C4 when forming complex **A** from **1** or complex **B** from complex **A**. In any case, it is clear from the data we have accumulated that transmetalation from **2** to palladium does not occur as the rds prior to attack at the thiophene. Rather, the thiophene must be involved in the rate-determining formation of complex **B**.

When invoking possible structures for complexes **A** and **B**, we arrive at a π complex of Pd^{II} to thiophene as the most likely structure for complex **A** (Figure 7). Structures of this type have been previously postulated^[18] when studying the interaction between palladium(II) salts and electron-rich heteroarenes. Our data do not provide further evidence for the precise structure (η^2 , η^4 , or η^5) nor for the ligand stoichiometry ($n=1,2$). In any case, $\text{Pd}(\text{tfa})_2$ acts as a Lewis acid in its association to the π -nucleophilic thiophene **1**. The equilibrium constant K_1 [Eq. (2)] is expected to be higher for electron-rich thiophenes, which could serve as one piece of evidence (see below) for the negative ρ value obtained from the Hammett plot.

Regarding the structure of complex **B**, previous work suggested that transmetalation from the arylboronic acid to palladium^[19,20] was favored over immediate attack of the arylboronic acid at the thiophene core.^[3c,9] The alternative structure, **B'**, would result from the latter event and would enable rapid *syn*- β -hydride elimination to the final product. For complex **B**, *anti*- β -hydride elimination,^[21] isomerization with subsequent *syn*- β -hydride elimination,^[22] or α -hydride elimination followed by a [1,2]-hydride shift^[23] would be required for a rapid carbometalation reaction to succeed.

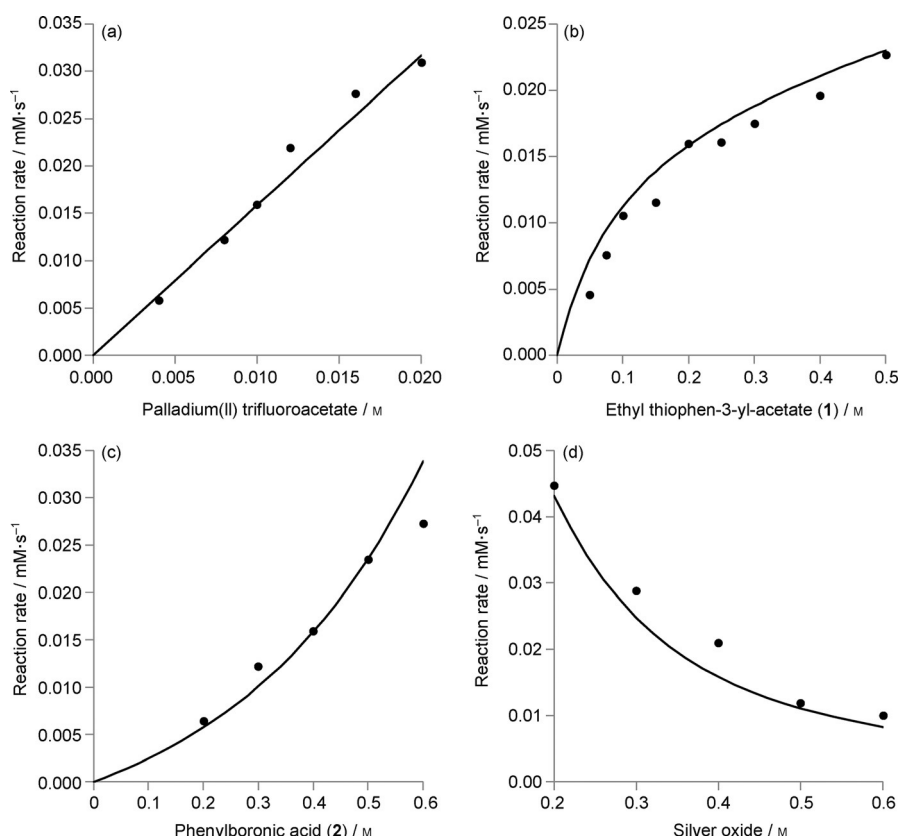


Figure 6. Experimental data (●) and best fit curves (—) calculated from the rate law.

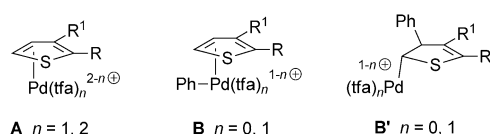


Figure 7. Possible structures of the putative intermediates **A**, **B**, and **B'** in the catalytic cycle (Scheme 5) of the oxidative cross-coupling.

Possible transition states that could lead to intermediates **B** or **B'** are depicted in Figure 8. For the formation of **B**, that is, for the transmetalation of the phenyl group, it is conceivable that the boron atom of **2** is simultaneously activated by the trifluoroacetate anion.^[20] An intramolecular reaction course can be envisioned for this process. If activation occurs prior to phenyl–palladium bond formation in **TS_B**, the palladium bears a positive partial charge in the transition state, which would account for the observed negative ρ value. In a similar fashion,

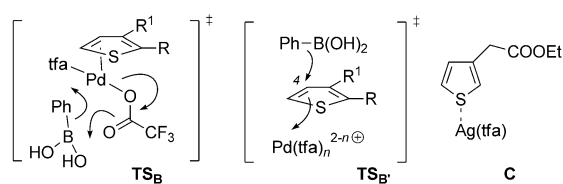


Figure 8. Possible transition states (**TSs**) leading to intermediates **B** ($n = 2$) or **B'** ($n = 1, 2$), as well as the tentative structure of complex **C**.

if palladium–carbon bond formation has significantly progressed in **TS_B** before attack of **2**, the partial positive charge at carbon atom C4 would be in line with the results of the Hammett analysis. It remains open for this transition state, however, how **2** is activated to render it sufficiently nucleophilic for the delivery of a phenyl group. There was no indication in any of our experiments that the trifluoroacetate concentration had a favorable influence on the reaction rate. If palladium was coordinated in complex **A** in an η^4 fashion, the sulfur atom could possibly act as a Lewis basic site to activate the boron atom.^[18b]

Although we have not collected further data on the composition of silver complexes **C** and **D**, it is possible to assign tentative structures to these complexes based on literature data. Complexation of thiophene to silver salts has been established by several crystal structures to occur through the sulfur atom.^[24] In line with these studies, we postulate that complex **C** formed from thiophene **1** and **Ag(tfa)** exhibit a similar coordinative bond (Figure 8). There is much less precedence for the association of Ag^+ to arylboronic acids or to other boronic acids. However, based on the limited data set available,^[25,26] it can be assumed that an association of **2** to silver occurs through at least one boronic acid oxygen atom. A chelate-type association with both oxygen atoms bound to silver is also conceivable.

After formation of complex **B**, all consecutive steps should be rapid. Possible reaction pathways to product **3** have already been mentioned and would generate palladium in its reduced state, that is, as palladium(0) (Scheme 5). Reoxidation to palladium(II) must therefore also occur in a fast process, possibly facilitated by **BQ** as a co-oxidant.^[27]

Conclusion

Kinetic studies on the oxidative palladium(II)-catalyzed cross-coupling between **2** and thiophenes have shown that not only palladium, but also **2** and the thiophene component, are involved in the rds of the reaction. This result is not in agreement with slow transmetalation from **2** to palladium nor with a slow reaction between a phenylpalladium intermediate and thiophene. Together with the other experimentally determined reaction orders and additional equilibrium studies, it implies a more complex mechanistic scenario. Moreover, it was found that the reaction showed no significant KIE at position C4 of

the thiophene core and that it exhibited a negative ρ value in a Hammett analysis. Based on these data, a tentative mechanistic model for the reaction was developed, which agreed with the observed reaction orders. In this model, a reversible association of thiophene to palladium is assumed to precede the reaction with **2**. It is unclear from our data whether **2** delivers the phenyl group in the rds to the palladium center (transmetalation) or directly to the thiophene core. Based on literature precedence, the former scenario seems, at this point in time, more likely than the latter.^[28]

When drawing conclusions from the experimental data, it should be kept in mind that, as stated in the Introduction, the large number of reaction ingredients extends significantly the mechanistic options. In this regard, the data we have accumulated can certainly be rationalized by alternative models. However, we feel that a continuing collection of kinetic data is required to increase our mechanistic understanding of C–H activation chemistry.

Experimental Section

Materials

Experiments with oxygen- or moisture-sensitive reagents were performed in flame-dried glassware under an argon atmosphere by using Schlenk techniques. Dry THF was obtained from an MBraun MB-SPS 800 solvent purification system. The following solvents were obtained from commercial sources, in the purities mentioned, and used without further purification: *tert*-butyl methyl ether (Grüssing, 99.5%), TFA (Sigma–Aldrich, ReagentPlus, 99%), acetic acid (Sigma–Aldrich, ReagentPlus, $\geq 99\%$), and toluene (Acros, 99.8%, Extra Dry, < 50 ppm H_2O). Technical solvents used for aqueous workup and purification by either crystallization or column chromatography (EtOAc, cyclohexane, Et_2O , pentane, hexane) were distilled prior to use. The following chemicals were obtained from commercial sources in the purities mentioned, and used without further purification: $\text{Pd}(\text{tfa})_2$ (Alfa-Aesar, 97%), Ag_2O (Alfa-Aesar, 99+%), $\text{Cs}(\text{tfa})$ (Alfa Aesar), **2** (Acros, 98+%), 2-phenylthiophene (ABCR, 95%), and **1** (Alfa-Aesar, 98%). BQ (Merck) was recrystallized from hexane.^[29]

Methods

TLC was performed on precoated glass-backed Kieselgel 60 F_{254} plates (Merck) with visualization effected through UV irradiation ($\lambda = 254, 366$ nm) and/or staining with a solution of potassium permanganate (3 g), potassium carbonate (20 g), and a 5% aqueous solution of sodium hydroxide (5 mL) in water (300 mL) with subsequent heating. Flash column chromatography with silica gel (230–400 mesh; Merck) was performed according to the method employed by Still et al.^[30] ^1H NMR spectra were recorded on Bruker AV-250, Bruker AV-360, or Bruker AV-500 spectrometers at 303 K. ^1H NMR spectra for the equilibrium studies were recorded on a Bruker AV-500-Cryo instrument. Data is reported in the following manner: chemical shift (in ppm relative to residual CHCl_3 ($\delta_{\text{H}} = 7.26$ ppm)), multiplicity, coupling constant J (measured in Hz to the nearest 0.1 Hz), and number of protons. The multiplicity of a signal is indicated as s=singlet, d=doublet, t=triplet, q=quartet, m=multiplet, or combinations of these. ^{13}C NMR spectra were recorded on the same Bruker AV-250, Bruker AV-360, or Bruker AV-500 spectrometers at 303 K operating at 63, 91, and 126 MHz, respec-

tively, with proton decoupling. The chemical shift (in ppm) is reported relative to residual CDCl_3 ($\delta_{\text{C}} = 77.16$ ppm). Structural assignments were made with the aid of DEPT 135, COSY, HSQC, HMBC, and NOESY experiments. IR spectra were recorded on a JASCO IR-4100 (ATR) spectrometer. Only selected characteristic bands are recorded. HRMS data were recorded on a Thermo Fischer Scientific DFS high-resolution mass spectrometer (HR-EI), or a Thermo Finnigan LTQ FT (HRMS-ESI) instrument, with each value obtained within 5 ppm of the calculated mass. GLC analysis was performed on an Agilent 6890 instrument (detector: FID) with an HP-5 column (30 m \times 0.25 mm ID, 0.25 μm). GLC-MS (EI) analysis was performed on an Agilent 6890 instrument (detector: 5973N MSD-EI; 70 eV) with an HP-5MS-UI column (30 m \times 0.25 mm ID, 0.25 μm). Method used for standard separation: STD (60 $^\circ\text{C}$ for 3 min, 15 $^\circ\text{C min}^{-1}$ \rightarrow 250 $^\circ\text{C}$, 250 $^\circ\text{C}$ for 5 min). The deuterium content was determined by using the selected-ion monitoring mode and considering the mass spectrum of each of the isotopomers.

General procedure for the determination of the initial rates for the kinetic studies

A solution of $\text{Pd}(\text{tfa})_2$ (50.0 μmol , 0.1 equiv), Ag_2O (1.00 mmol, 2.0 equiv), BQ (250 μmol , 0.5 equiv), and $\text{Cs}(\text{tfa})$ (500 μmol , 1.0 equiv) in TFA (2.5 mL) was stirred at 500 rpm for 5 min in a double-jacket round-bottomed flask. The suspension was treated in an ultrasonic bath for 2 min. The solution was tempered at 25 $^\circ\text{C}$ for 3 min. Boronic acid **2** (1.00 mmol, 2.0 equiv) was added and the reaction mixture was stirred for further 4 min. Benzyl acetate (140 μmol , 0.28 equiv) was added as an internal standard for GLC analysis, and the reaction was started with the rapid addition of **1** (500 μmol , 1.0 equiv). Aliquots (50 μL) of the reaction mixtures were taken every 2.00 min in a 5 mL vial containing *tert*-butyl methyl ether (2.0 mL). The solution was extracted immediately with an aqueous solution of sodium hydroxide (1.0 M, 0.60 mL); the organic layer was separated and analyzed by GLC.

General procedure for the 4-phenylation of thiophenes

A solution of $\text{Pd}(\text{tfa})_2$ (50.0 μmol , 0.1 equiv), Ag_2O (1.00 mmol, 2.0 equiv), BQ (250 μmol , 0.5 equiv), and $\text{Cs}(\text{tfa})$ (500 μmol , 1.0 equiv) in a mixture of TFA and HOAc (40:60 v/v; 2.5 mL) was stirred at 500 rpm for 5 min. The suspension was treated in an ultrasonic bath for 2 min. Boronic acid **2** (1.00 mmol, 2.0 equiv) and thiophene (500 μmol , 1.0 equiv) were added and the reaction mixture was stirred at room temperature for 1–15 h. The reaction mixture was diluted with diethyl ether (40 mL) and neutralized with an aqueous solution of potassium carbonate (20 wt%; 20 mL). The aqueous layer was extracted with diethyl ether (2 \times 40 mL). The combined organic layers were washed with a saturated aqueous solution of sodium chloride (20 mL), dried over MgSO_4 , filtered, and concentrated in vacuo. Purification of the residue by flash column chromatography yielded the corresponding 4-phenylated thiophenes.

Procedure for the analysis of the KIE

A solution of $\text{Pd}(\text{tfa})_2$ (16.6 mg, 50.0 μmol , 0.1 equiv), Ag_2O (232 mg, 1.00 mmol, 2.0 equiv), BQ (27.0 mg, 250 μmol , 0.5 equiv), and $\text{Cs}(\text{tfa})$ (123 mg, 500 μmol , 1.0 equiv) in TFA (2.5 mL) was stirred at 500 rpm for 5 min. The suspension was treated in an ultrasonic bath for 2 min. Boronic acid **2** (122 mg, 1.00 mmol, 2.0 equiv) was added and the reaction mixture was stirred for further 4 min. Benzyl acetate (20.0 μL , 21.1 mg, 140 mmol, 0.28 equiv) was added as an internal standard for GLC analysis, and the reac-

tion was started with the rapid addition of both isotopes of **1** and $[4\text{-D}_1]\mathbf{1}$ (250 μmol each). Aliquots (50 μL) of the reaction mixtures were taken every 30 min in a 5 mL vial containing *tert*-butyl methyl ether (2.0 mL). The solution was extracted immediately with an aqueous solution of sodium hydroxide (1.0 M, 0.60 mL); the organic layer was separated and analyzed with GLC and GLC-MS.

3-Bromo-4-deuteriothiophene (**4**)

Following a procedure by Wagner et al.,^[31] a solution of 3,4-dibromothiophene (5.00 g, 20.7 mmol, 1.0 equiv) in dry THF (25 mL) was cooled to 0 °C with an ice bath. *i*PrMgCl (13.0 mL, 1.83 M (THF), 23.8 mmol, 1.15 equiv) was added over a period of 30 min and the reaction mixture was stirred for further 1 h. A mixture of D₂O (5 mL) and D₂SO₄ (1 mL) was added slowly. The solution was concentrated, water (20 mL) was added, and the aqueous layer was extracted with diethyl ether (3 \times 20 mL). The combined organic layers were dried over MgSO₄, filtered, and concentrated in vacuo. After purification by flash column chromatography (\varnothing = 7.0 cm, *l* = 15 cm, pentane), product **4** was obtained as a colorless liquid (3.35 g, 20.4 mmol, 99%). ¹H NMR (500 MHz, C₆D₆): δ = 6.68 (d, ⁴*J* = 3.2 Hz, 1H), 6.51 ppm (d, ⁴*J* = 3.2 Hz, 1H); ¹³C NMR (126 MHz, C₆D₆): δ = 129.4 (t, ¹*J*(C,D) = 26.6 Hz), 126.3, 122.6, 109.8 ppm; MS (EI, 70 eV): *m/z* (%): 165 (100) [*M*^{(81)Br}]⁺, 163 (100) [*M*^{(79)Br}]⁺, 84 (40) [*M*–Br]⁺.

Diethyl 2-(4-deuteriothiophen-3-yl)malonate (**5**)

Following a procedure by Gooßen et al.,^[32] a Schlenk tube with a Teflon screw cap was charged with Pd(dba)₂ (92.0 mg, 160 μmol , 0.02 equiv), P(*t*Bu)₃·HBF₄ (102 mg, 350 μmol , 0.044 equiv), and K₂CO₃ (2.21 g, 16.0 mmol, 2.0 equiv). The reaction vessel was evacuated and backfilled with argon three times. Degassed diethyl malonate (4.0 mL) and 3-bromo-4-deuteriothiophene (**4**; 1.31 g, 8.00 mmol, 1.0 equiv) were added under an argon countercurrent and the reaction mixture was stirred at 90 °C for 5 h. Water (20 mL) was added and the resulting mixture was extracted with diethyl ether (2 \times 20 mL). The combined organic layers were dried over MgSO₄, filtered, and concentrated in vacuo. After purification by Kugelrohr distillation, product **5** was obtained as a colorless liquid (2.06 g, 4.49 mmol, 56%), which contained an additional 47% diethyl malonate as an impurity. From the lower boiling fraction, starting material **4** (164 mg, 1.00 mmol, 13%) was recovered after flash column chromatography (hexane). The product was converted without further purification. ¹H NMR (500 MHz, C₆D₆): δ = 7.13 (d, ⁴*J* = 3.0 Hz, 1H), 6.84 (d, ⁴*J* = 3.0 Hz, 1H), 4.71 (s, 1H), 3.85–3.93 (m, 4H), 0.86 ppm (t, ³*J* = 7.3 Hz, 6H); ¹³C NMR (126 MHz, C₆D₆): δ = 167.7, 133.0, 128.4 (t), 125.6, 124.7, 61.6, 53.8, 13.9 ppm; MS (EI, 70 eV): *m/z* (%): 243 (75) [*M*⁺], 170 (100), 142 (35), 125 (35), 114 (40), 98 (75), 86 (30).

Ethyl 2-(4-deuteriothiophen-3-yl)acetate [4-D₁](**1**)

Following a procedure by Krapcho et al.,^[13] a solution of crude diethyl 2-(4-deuteriothiophen-3-yl)malonate (**5**; 2.06 g, 4.48 mmol, 1.0 equiv) and sodium hydroxide (500 mg, 8.55 mmol, 1.9 equiv) in a mixture of water and DMSO (1/20 v/v; 10.5 mL) was heated at 160 °C for 5 h. After cooling to room temperature, water (50 mL) was added and the aqueous layer was extracted with diethyl ether (3 \times 20 mL). The combined organic layers were dried over MgSO₄, filtered, and concentrated in vacuo. After purification by flash column chromatography (hexane/Et₂O 9:1), product [4-D₁]**1** was obtained as a colorless liquid (675 mg, 3.94 mmol, 88%). A purity of 99% and a deuterium content of 99% were determined by GLC

and GLC-MS in accordance with ¹H NMR spectroscopy measurements. ¹H NMR (500 MHz, C₆D₆): δ = 6.86 (d, ⁴*J* = 3.0 Hz, 1H), 6.82 (d, ⁴*J* = 3.0 Hz, 1H), 3.88 (q, ³*J* = 7.2 Hz, 2H), 3.32 (s, 2H), 0.89 ppm (t, ³*J* = 7.2 Hz, 3H); ¹³C NMR (126 MHz, C₆D₆): δ = 170.4, 134.2, 128.6 (t, ¹*J*(C,D) = 25.7 Hz), 125.6, 122.9, 60.6, 35.9, 14.2 ppm; IR (ATR): $\tilde{\nu}$ = 3105, 2980, 2935, 1730, 1365, 1300, 1255, 1185, 1135, 1030, 865, 810, 725 cm^{–1}; MS (EI, 70 eV): *m/z* (%): 171 (35) [*M*⁺], 98 (100); HRMS (EI, 70 eV): *m/z* calcd for C₈H₉DO₂³²S [*M*⁺]: 171.0459; found: 171.0459.

General procedure for the determination of the relative rate constants for Hammett analysis

A solution of Pd(tfa)₂ (50.0 μmol , 0.1 equiv), Ag₂O (1.00 mmol, 2.0 equiv), BQ (250 μmol , 0.5 equiv), and Cs(tfa) (500 μmol , 1.0 equiv) in a mixture of TFA and HOAc (40:60 v/v; 2.5 mL) was stirred at 500 rpm for 5 min. The suspension was treated in an ultrasonic bath for 2 min. Boronic acid **2** (1.00 mmol, 2.0 equiv) was added and stirring was continued for a further 5 min. The reaction was started by the rapid addition of the competing thiophene substrates (0.25 mmol each) and benzyl acetate (140 μmol , 0.28 equiv; internal standard for GLC analysis) as a solution in CH₂Cl₂ (50 μL). Aliquots (50 μL) of the reaction mixtures were taken every 2 min in a 5 mL vial containing *tert*-butyl methyl ether (2.0 mL). The solution was extracted immediately with an aqueous solution of sodium hydroxide (1.0 M, 0.60 mL); the organic layer was separated and analyzed with GLC.

(*E*)-Stilbene (**9**)

Following the general procedure for the 4-phenylation of thiophenes, compound **8** (57 μL , 52 mg, 0.50 mmol, 1.0 equiv) instead of thiophene was used and the reaction mixture was stirred at room temperature for 2.5 h. After purification by flash column chromatography (hexane), product **9** was obtained as a colorless solid (66 mg, 370 μmol , 73%) as a single isomer. ¹H NMR (250 MHz, CDCl₃): δ = 7.55–7.60 (m, 4H), 7.38–7.45 (m, 4H), 7.28–7.35 (m, 2H), 7.17 ppm (s, 2H); ¹³C NMR (63 MHz, CDCl₃): δ = 137.5, 128.8, 128.8, 127.7, 126.6 ppm.

Acknowledgements

This work was supported by the graduate college NanoCat (scholarship to I.S.), the TUM Graduate School, and the Fonds der Chemischen Industrie. T.B. conceived and directed the synthetic aspects of the project, with I.S. performing all synthetic work. S.B. devised and analyzed the kinetic studies. S.B. and T.B. composed the manuscript.

Keywords: C–H activation • cross-coupling • heterocycles • kinetics • palladium

- [1] For reviews and monographs, see: a) D. Alberico, M. E. Scott, M. Lautens, *Chem. Rev.* **2007**, *107*, 174–238; b) I. V. Seregin, V. Gevorgyan, *Chem. Soc. Rev.* **2007**, *36*, 1173–1193; c) L. Ackermann, *Modern Arylation Methods*, Wiley-VCH, Weinheim **2009**; d) X. Chen, K. M. Engle, D.-H. Wang, J.-Q. Yu, *Angew. Chem. Int. Ed.* **2009**, *48*, 5094–5115; *Angew. Chem.* **2009**, *121*, 5196–5217; e) L. Ackermann, R. Vicente, A. R. Kapdi, *Angew. Chem. Int. Ed.* **2009**, *48*, 9792–9826; *Angew. Chem.* **2009**, *121*, 9976–10011; f) F. Bellina, R. Rossi, *Tetrahedron* **2009**, *65*, 10269–10310; g) C.-L. Sun, B.-J. Li, Z.-J. Shi, *Chem. Commun.* **2010**, *46*, 677–685; h) J. Roger, A. L. Gottumukkala, H. Doucet, *ChemCatChem* **2010**, *2*, 20–40;

- i) W. Shi, C. Liu, A. Lei, *Chem. Soc. Rev.* **2011**, *40*, 2761–2776; j) N. Kuhl, M. N. Hopkinson, J. Wencel-Delord, F. Glorius, *Angew. Chem. Int. Ed.* **2012**, *51*, 10236–10254; *Angew. Chem.* **2012**, *124*, 10382–10401; k) R. Rossi, F. Bellina, M. Lessi, C. Manzini, *Adv. Synth. Catal.* **2014**, *356*, 17–117; l) I. Hussain, T. Singh, *Adv. Synth. Catal.* **2014**, *356*, 1661–1696.
- [2] For selected contributions to the palladium-catalyzed arylation of thiophenes and benzothiophenes with aryl halides, see: a) C. Gozzi, L. Lave-not, K. Ilg, V. Penalva, M. Lemaire, *Tetrahedron Lett.* **1997**, *38*, 8867–8870; b) B. Glover, K. A. Harvey, B. Liu, M. J. Sharp, M. F. Tymoschenko, *Org. Lett.* **2003**, *5*, 301–304; c) B. Liégault, D. Lapointe, L. Caron, A. Vlasova, K. Fagnou, *J. Org. Chem.* **2009**, *74*, 1826–1834; d) S. Yanagisawa, K. Ueda, H. Sekizawa, K. Itami, *J. Am. Chem. Soc.* **2009**, *131*, 14622–14623; e) K. Ueda, S. Yanagisawa, J. Yamaguchi, K. Itami, *Angew. Chem. Int. Ed.* **2010**, *49*, 8946–8949; *Angew. Chem.* **2010**, *122*, 9130–9133; f) D. Roy, S. Mom, M. Beaupérin, H. Doucet, J.-C. Hierro, *Angew. Chem. Int. Ed.* **2010**, *49*, 6650–6654; *Angew. Chem.* **2010**, *122*, 6800–6804; g) J. J. Dong, H. Doucet, *Eur. J. Org. Chem.* **2010**, 611–615; h) H. Kamiya, S. Yanagisawa, S. Hiroto, K. Itami, H. Shinokubo, *Org. Lett.* **2011**, *13*, 6394–6397; i) L. Chen, J. Roger, C. Bruneau, P. H. Dixneuf, H. Doucet, *Chem. Commun.* **2011**, 1872–1874; j) J. J. Dong, D. Roy, R. J. Roy, M. Ionita, H. Doucet, *Synthesis* **2011**, 3530–3546; k) D. J. Schipper, K. Fagnou, *Chem. Mater.* **2011**, *23*, 1594–1600; l) D. Ghosh, H. M. Lee, *Org. Lett.* **2012**, *14*, 5534–5537; m) C. B. Bheeter, J. K. Bera, H. Doucet, *RSC Adv.* **2012**, *2*, 7197–7206; n) L. Chen, C. Bruneau, P. H. Dixneuf, H. Doucet, *Tetrahedron* **2013**, *69*, 4381–4388; o) R. Jin, B. Bheeter, H. Doucet, *Beilstein J. Org. Chem.* **2014**, *10*, 1239–1245; p) T. Dao-Huy, M. Haider, F. Glatz, M. Schnürch, M. D. Mihovilovic, *Eur. J. Org. Chem.* **2014**, 8119–8125; q) R. Matsidik, J. Martin, S. Schmidt, J. Obermayer, F. Lombeck, F. Nübling, H. Komber, D. Fazzi, M. Sommer, *J. Org. Chem.* **2015**, *80*, 980–987.
- [3] For selected contributions to the palladium-catalyzed arylation of thiophenes and benzothiophenes by oxidative cross-coupling with arylboronic acids, see: a) S.-D. Yang, C.-L. Sun, Z. Fang, B.-J. Li, Y.-Z. Li, Z.-J. Shi, *Angew. Chem. Int. Ed.* **2008**, *47*, 1473–1476; *Angew. Chem.* **2008**, *120*, 1495–1498; b) S. Kirchberg, T. Vogler, A. Studer, *Synlett* **2008**, 2841–2845; c) S. Kirchberg, S. Tani, K. Ueda, J. Yamaguchi, A. Studer, K. Itami, *Angew. Chem. Int. Ed.* **2011**, *50*, 2387–2391; *Angew. Chem.* **2011**, *123*, 2435–2439; d) K. Yamaguchi, J. Yamaguchi, A. Studer, K. Itami, *Chem. Sci.* **2012**, *3*, 2165–2169; e) R. Srinivasan, R. S. Kumaran, N. S. Nagarajan, *RSC Adv.* **2014**, *4*, 47697–47700; f) Z. Wang, Y. Li, B. Yan, M. Huang, Y. Wu, *Synlett* **2015**, 531–536.
- [4] For kinetic studies on C–H activation reactions at arenes, see: a) L. J. Ackerman, J. P. Sadighi, D. M. Kurtz, J. A. Labinger, J. E. Bercaw, *Organometallics* **2003**, *22*, 3884–3890; b) B. S. Lane, M. A. Brown, D. Sames, *J. Am. Chem. Soc.* **2005**, *127*, 8050–8057; c) K. L. Hull, M. S. Sanford, *J. Am. Chem. Soc.* **2009**, *131*, 9651–9653; d) H.-Y. Sun, S. I. Gorelsky, D. R. Stuart, L.-C. Campeau, K. Fagnou, *J. Org. Chem.* **2010**, *75*, 8180–8189; e) Y. Tan, F. Barrios-Landeros, J. F. Hartwig, *J. Am. Chem. Soc.* **2012**, *134*, 3683–3686; f) R. D. Baxter, D. Sale, K. M. Engle, J.-Q. Yu, D. G. Blackmond, *J. Am. Chem. Soc.* **2012**, *134*, 4600–4606; g) K. C. Pereira, A. L. Porter, S. Potavathri, A. P. LeBris, B. DeBoef, *Tetrahedron* **2013**, *69*, 4429–4435; h) D. Wang, Y. Izawa, S. S. Stahl, *J. Am. Chem. Soc.* **2014**, *136*, 9914–9917; i) D. E. Stephens, J. Lakey-Beitia, A. C. Atesin, T. A. Atesin, G. Chavez, H. D. Arman, O. V. Larionov, *ACS Catal.* **2015**, *5*, 167–175; j) A. K. Cook, M. S. Sanford, *J. Am. Chem. Soc.* **2015**, *137*, 3109–3118.
- [5] I. Schnapperelle, S. Breitenlechner, T. Bach, *Org. Lett.* **2011**, *13*, 3640–3643.
- [6] For regioselective oxidative cross-coupling reactions at thiophenes, unless mentioned in ref. [3], see: a) K. Funaki, T. Sato, S. Oi, *Org. Lett.* **2012**, *14*, 6186–6189; b) M. Murai, K. Takami, K. Takai, *Chem. Eur. J.* **2015**, *21*, 4566–4570.
- [7] I. Schnapperelle, T. Bach, *ChemCatChem* **2013**, *5*, 3232–3236.
- [8] I. Schnapperelle, T. Bach, *Chem. Eur. J.* **2014**, *20*, 9725–9732.
- [9] M. Steinmetz, K. Ueda, S. Grimme, J. Yamaguchi, S. Kirchberg, K. Itami, A. Studer, *Chem. Asian J.* **2012**, *7*, 1256–1260.
- [10] For related computational results, see: S.-Y. Tang, Q.-X. Guo, Y. Fu, *Chem. Eur. J.* **2011**, *17*, 13866–13876.
- [11] a) K. J. Hall, T. I. Quickenden, D. W. Watts, *J. Chem. Educ.* **1976**, *53*, 493–494; b) J. Casado, M. A. López-Quintela, F. M. Lorenzo-Barral, *J. Chem. Educ.* **1986**, *63*, 450–452.
- [12] Reviews: a) L. Fielding, *Tetrahedron* **2000**, *56*, 6151–6170; b) J. S. Renny, L. L. Tomasevich, E. H. Tallmadge, D. B. Collum, *Angew. Chem. Int. Ed.* **2013**, *52*, 11998–12013; *Angew. Chem.* **2013**, *125*, 12218–12234.
- [13] A. P. Krapcho, J. F. Weimaster, J. M. Eldridge, E. G. E. Jahngen, Jr., A. J. Lovey, W. P. Stephens, *J. Org. Chem.* **1978**, *43*, 138–147.
- [14] a) M. Gómez-Gallego, M. A. Sierra, *Chem. Rev.* **2011**, *111*, 4857–4963; b) E. M. Simmons, J. F. Hartwig, *Angew. Chem. Int. Ed.* **2012**, *51*, 3066–3072; *Angew. Chem.* **2012**, *124*, 3120–3126.
- [15] a) C. Hansch, A. Leo, R. W. Taft, *Chem. Rev.* **1991**, *91*, 165–195; b) F. A. Carey, R. J. Sundberg, *Advanced Organic Chemistry, Part A: Structure and Mechanisms*, Kluwer Academic/Plenum Publishers, New York, **2000**, pp. 204–215; c) H. Man Yau, A. K. Croft, J. B. Harper, *Chem. Commun.* **2012**, 48, 8937–8939.
- [16] For a review, see: B. Karimi, H. Behzadnia, D. Elhamifar, P. F. Akhavan, F. K. Esfahani, A. Zamani, *Synthesis* **2010**, 1399–1427.
- [17] a) L. Michaelis, M. L. Menten, *Biochem. Z.* **1913**, *49*, 333–369; b) G. E. Briggs, J. B. S. Haldane, *Biochem. J.* **1925**, *19*, 338–339; c) K. A. Johnson, R. S. Goody, *Biochemistry* **2011**, *50*, 8264–8269.
- [18] a) M. J. H. Russell, C. White, A. Yates, P. M. Maitlis, *J. Chem. Soc. Dalton Trans.* **1978**, 857–861; b) R. J. Angelici, *Coord. Chem. Rev.* **1990**, *105*, 61–76; c) D.-L. Wang, W.-S. Hwang, *J. Organomet. Chem.* **1991**, *406*, C29–C32.
- [19] For a review, see: D. V. Partyka, *Chem. Rev.* **2011**, *111*, 1529–1595.
- [20] For the transmetalation of arylboronic acids to palladium, see: a) M. Moreno-Mañas, M. Pérez, R. Pleixats, *J. Org. Chem.* **1996**, *61*, 2346–2351; b) L. J. Goossen, D. Koley, H. L. Hermann, W. Thiel, *J. Am. Chem. Soc.* **2005**, *127*, 11102–11114; c) A. A. C. Braga, N. H. Morgon, G. Ujaque, F. Maseras, *J. Am. Chem. Soc.* **2005**, *127*, 9298–9307; d) H. Ohmiya, Y. Makida, D. Li, M. Tanabe, M. Sawamura, *J. Am. Chem. Soc.* **2010**, *132*, 879–889; e) B. P. Carrow, J. F. Hartwig, *J. Am. Chem. Soc.* **2011**, *133*, 2116–2119; f) M. Iwasaki, Y. Nishihara, in *Applied Cross-Coupling Reactions* (Ed.: Y. Nishihara), Springer, Heidelberg, **2013**, pp. 17–28; g) A. J. J. Lennox, G. C. Lloyd-Jones, *Angew. Chem. Int. Ed.* **2013**, *52*, 7362–7370; *Angew. Chem.* **2013**, *125*, 7506–7515; h) C. Amatore, G. Le Duc, A. Jutand, *Chem. Eur. J.* **2013**, *19*, 10082–10093; i) A. R. Kapdi, G. Dhangar, J. L. Serrano, J. Pérez, L. García, I. J. S. Fairlamb, *Chem. Commun.* **2014**, 50, 9859–9861; j) G. Audran, P. Brémond, S. R. A. Marque, D. Siri, M. Santelli, *Tetrahedron* **2014**, *70*, 2272–2279.
- [21] a) J. M. Takacs, E. C. Lawson, F. Clement, *J. Am. Chem. Soc.* **1997**, *119*, 5956–5957; b) N. J. Adams, J. Bargon, J. M. Brown, E. J. Farrington, E. Galardon, R. Giernoth, H. Heinrich, B. D. John, K. Maeda, *Pure Appl. Chem.* **2001**, *73*, 343–346; c) K. Maeda, E. J. Farrington, E. Galardon, B. D. John, J. M. Brown, *Adv. Synth. Catal.* **2002**, *344*, 104–109; d) M. Lautens, Y.-Q. Fang, *Org. Lett.* **2003**, *5*, 3679–3682; e) S.-Y. Tang, J. Zhang, Y. Fu, *Comput. Theor. Chem.* **2013**, *1007*, 31–40.
- [22] a) K. S. Y. Lau, P. K. Wong, J. K. Stille, *J. Am. Chem. Soc.* **1976**, *98*, 5832–5840; b) K. L. Granberg, J.-E. Bäckvall, *J. Am. Chem. Soc.* **1992**, *114*, 6858–6863; c) K. M. Shea, K. L. Lee, R. L. Danheiser, *Org. Lett.* **2000**, *2*, 2353–2356.
- [23] a) C. A. Busacca, J. Swestock, R. E. Johnson, T. R. Bailey, L. Musza, C. A. Rodger, *J. Org. Chem.* **1994**, *59*, 7553–7556; b) V. Farina, M. A. Hossain, *Tetrahedron Lett.* **1996**, *37*, 6997–7000.
- [24] For examples, see: a) G. C. van Stein, G. van Koten, A. L. Spek, A. J. M. Duisenberg, E. A. Klop, *Inorg. Chim. Acta* **1983**, *78*, L61–L63; b) G. C. van Stein, G. van Koten, F. Blank, L. C. Taylor, K. Vrieze, A. L. Spek, A. J. M. Duisenberg, A. M. M. Schreurs, B. Kojić-Prodić, C. Brevard, *Inorg. Chim. Acta* **1985**, *98*, 107–120; c) J. F. Modder, J.-M. Ernsting, K. Vrieze, M. de Wit, C. H. Stam, G. van Koten, *Inorg. Chem.* **1991**, *30*, 1208–1214; d) H. Konaka, L. P. Wu, M. Munakata, T. Kuroda-Sowa, M. Maekawa, Y. Suenaga, *Inorg. Chem.* **2003**, *42*, 1928–1934; e) M. Ghassemzadeh, A. Sharifi, J. Malakootikhah, B. Neumüller, E. Iravani, *Inorg. Chim. Acta* **2004**, *357*, 2245–2252.
- [25] a) B. A. Arbuzov, G. N. Nikonov, A. A. Karasik, K. M. Enikeev, *Bull. Acad. Sci. USSR Div. Chem. Sci. (Engl. Transl.)* **1991**, *40*, 804–809; b) D.-Z. Li, C.-C. Dong, S.-G. Zhang, *J. Mol. Model.* **2013**, *19*, 3219–3224.
- [26] An association of the trifluoroacetate anion to **2** in complex **D** seems unlikely. Na(tfa) addition to **2** did not result in any chemical shift changes in the ¹H NMR spectrum.
- [27] For a recent review, see: A. Vasseur, J. Muzart, J. Le Bras, *Eur. J. Org. Chem.* **2015**, 4053–4069.

- [28] Preliminary DFT calculations on model systems indicate that there is a viable reaction pathway for transmetalation via a transition state related to **TS_B**. Transition state **TS_B** or related transition states could not be located computationally: S. M. Huber, T. Bach, unpublished results.
- [29] W. L. F. Armarego, C. L. L. Chai, *Purification of Laboratory Chemicals*, Butterworth–Heinemann, Amsterdam, **2009**, p. 241.
- [30] W. C. Still, M. Kahn, A. Mitra, *J. Org. Chem.* **1978**, *43*, 2923.
- [31] R. Wagner, P. L. Donner, D. J. Kempf, C. J. Maring, V. S. Stoll, Y.-Y. Ku, Y.-M. Pu (Abbott Laboratories), WO2008011337A1, **2008**.
- [32] B. Song, F. Rudolphi, T. Himmler, L. J. Gooßen, *Adv. Synth. Catal.* **2011**, *353*, 1565–1574.

Received: August 4, 2015

Published online on October 30, 2015
